



ELSEVIER

Contents lists available at ScienceDirect

Biosensors and Bioelectronics

journal homepage: www.elsevier.com/locate/bios

Immunosensor for the ultrasensitive and quantitative detection of bladder cancer in point of care testing

Cheng-Hsin Chuang^{a,*}, Yi-Chun Du^b, Ting-Feng Wu^c, Cheng-Ho Chen^d, Da-Huei Lee^e, Shih-Min Chen^a, Ting-Chi Huang^a, Hsun-Pei Wu^a, Muhammad Omar Shaikh^a

^a Department of Mechanical Engineering, Southern Taiwan University of Science and Technology, Tainan 71005, Taiwan

^b Department of Electrical Engineering, Southern Taiwan University of Science and Technology, Tainan 71005, Taiwan

^c Department of Biotechnology, Southern Taiwan University of Science and Technology, Tainan 71005, Taiwan

^d Department of Chemistry and Material Engineering, Southern Taiwan University of Science and Technology, Tainan 71005, Taiwan

^e Department of Electronic Engineering, Southern Taiwan University of Science and Technology, Tainan 71005, Taiwan

ARTICLE INFO

Article history:

Received 23 September 2015

Received in revised form

22 December 2015

Accepted 29 December 2015

Available online 30 December 2015

Keywords:

Immunosensor

Impedance

Microelectrodes

Dielectrophoresis

Point of care

ABSTRACT

An ultrasensitive and real-time impedance based immunosensor has been fabricated for the quantitative detection of Galectin-1 (Gal-1) protein, a biomarker for the onset of multiple oncological conditions, especially bladder cancer. The chip consists of a gold annular interdigitated microelectrode array (3×3 format with a sensing area of $200 \mu\text{m}$) patterned using standard microfabrication processes, with the ability to electrically address each electrode individually. To improve sensitivity and immobilization efficiency, we have utilized nanoprobe (Gal-1 antibodies conjugated to alumina nanoparticles through silane modification) that are trapped on the microelectrode surface using programmable dielectrophoretic manipulations. The limit of detection of the immunosensor for Gal-1 protein is 0.0078 mg/ml of T24 (Grade III) cell lysate in phosphate buffered saline, artificial urine and human urine samples. The normalized impedance variations show a linear dependence on the concentration of cell lysate present while specificity is demonstrated by comparing the immunosensor response for two different grades of bladder cancer cell lysates. We have also designed a portable impedance analyzing device to connect the immunosensor for regular checkup in point of care testing with the ability to transfer data over the internet using a personal computer. We believe that this diagnostic system would allow for improved public health monitoring and aid in early cancer diagnosis.

© 2015 Elsevier B.V. All rights reserved.

1. Introduction

Bladder cancer is the most common malignancy of the urinary tract with a very high recurrence rate even after treatment (Ploeg et al., 2009). Although cystoscopy remains the gold standard in detection and surveillance of bladder cancer, small papillary tumors or carcinoma in situ (CIS) can often be missed and may account for early recurrence. While there have been many molecular urinary tests developed, none have really been able to achieve required sensitivity or specificity to replace cystoscopy (Yutkin et al., 2010). The development of a non-invasive and reliable method for bladder cancer risk determination and early diagnosis would allow physicians to more effectively monitor disease progression, regression and recurrence. Furthermore, use of portable and automated systems for sensitive and quantitative sample to answer analysis in point of care combined with data transmission

for cloud computing will revolutionize cancer diagnosis and therapy.

In recent years, immunoassays have attracted widespread interest because they can achieve rapid, inexpensive and sensitive detection of the specific binding of an antigen to its corresponding antibody to form a stable complex (Ploeg et al., 2009; Yutkin et al., 2010; Daniels and Pourmand, 2007). Among the different types of transduction methods utilized in immunosensors, electrical/electrochemical detection provides label free analysis with reduction of complexity in signal acquisition while solely relying on the measurement of current and/or voltage to detect binding (Thévenot et al., 2001; Drummond et al., 2003). They possess an innate high sensitivity and simplicity and can be effectively integrated with miniaturized hardware which makes them arguably the most practical and quantifiable diagnostic technique for detection of proteins (Park et al., 2002; Zheng et al., 2005; Chikka-veeraiah et al., 2012). Impedance based electrical transduction, unlike amperometric or voltametric approaches, is performed in AC steady state with a constant DC bias and can thus be used to analyze both the resistive and the capacitive changes at the

* Corresponding author.

E-mail address: chchuang@mail.stust.edu.tw (C.-H. Chuang).

electrode surface over a wide frequency range during immunoreaction.

This analytical approach, known as electrochemical impedance spectroscopy (EIS), is an effective mediator free strategy for the non-destructive probing of complex bio-recognition events (Lisdatt and Schafer, 2008; Singh and Suni, 2010) and has wide applicability in biosensors for bacteria and pathogen detection to immunosensing and DNA characterization (Li et al., 2014; Elshafey et al., 2013; Ma et al., 2013). The electrical/biological interface in EIS, which largely dictates assay sensitivity, selectivity and stability, critically depends on the immobilization efficiency of recognition elements to a native or pre-modified electrode surface (Luo and Davis, 2013). Commonly used receptor immobilization methodologies are based on either physical (Hirsh et al., 2010) (electrostatic, ionic or hydrophobic interactions) or covalent coupling (self-assembled monolayers (SAMs) and carboxyl or amine derived chemistries (Shi and Ma, 2011; Rodriguez et al., 2005)). While SAMs and other layer by layer deposition techniques offer advantages like irreversible binding, high surface coverage and complete blocking capabilities and stabilities, perturbation and cross-contamination effects are difficult to control, especially when performing multiplexing in a micron scale detection area.

DEP has been used as an alternative technique for controllable, selective and accurate manipulation of a wide variety of bioreceptors onto the surface of the electrode sensing platform (Wlodkovic and Cooper, 2010; Zhang et al., 2010). In our previous works, we have utilized programmable three step DEP manipulations to effectively distinguish bladder cancer staging using multiple biomarkers on a single lab on a chip (LOC) device (Chuang et al., 2015). We have also shown that multiple microelectrodes in an array can be electrically addressed individually and the fluorescence response after immunosensing is significantly higher when DEP is utilized (Rodriguez et al., 2005). Microelectrodes significantly improve sensitivity, especially in low conductivity solutions, as they have a spherical diffusion profile that allows for rapid reaction kinetics with an improved signal to noise ratio (Radke and Alcolija, 2005; Harrington and Anderson, 1990). Furthermore, they enable the miniaturization of the detector device and the sample volume used.

In this study, we have fabricated a simple immunosensor chip that allows for ultrasensitive detection of Gal-1 without the use of complicated fluid handling using external devices. Recent proteomics investigations have shown that an overexpression of Gal-1 is a possible independent factor for bladder cancer prognosis (Wu et al., 2015). We have tried to amplify signal output by using antibody conjugated nanoparticles (nanoprobes) which allow enhanced surface areas while DEP has been used to increase the concentration of trapped nanoprobes at the microelectrode surface. The immunosensor can sensitively and specifically detect Gal-1 protein from a complex fluid like cell lysate and provides real time detection while only needing a sample volume in the microlitre range. We have also designed a prototype portable impedance analyzer based on the AD5933 IC into which the immunosensor can be inserted and quantitative analysis can be obtained. The integration of bioanalytical devices with portable or inbuilt data processing systems that can transmit the data wirelessly for further analysis will allow for improved point of care diagnostics.

2. Materials and methods

2.1. Surface modified nanoparticle synthesis

The nanoprobes are prepared using a two-step method which involves surface modification of the alumina nanoparticles

(Al₂O₃-NPs) followed by conjugation with the Gal-1 antibody. Commercially available Al₂O₃-NPs (AEROXIDE[®] Alu C, Evonik Degussa) with an average diameter of 50 nm were surface modified with amino groups using a 3-aminopropyltrimethoxysilane (MERCK) solution. In a typical process, 3 g of ethanol (95 wt%), 1.5 g of DI water and 1.25 g of silane solution were mixed under magnetic stirring at room temperature for 3 h. Next, 2.7 g Al₂O₃-NPs in 100 g of ethanol was added and the two solutions were mixed at 70 °C for 3 h. The functionalized nanoparticles were collected by centrifuging three times at 4000 rpm for 10 min. The sedimentary nanoparticles were baked at 60 °C for 12 h and the silane modified Al₂O₃-NPs can then be used for antibody conjugation.

2.2. Antibody conjugation

Before conjugation, the Gal-1 antibody was first oxidized in a solution containing 1 mM of sodium metaperiodate and 0.1 M sodium acetate with the pH maintained at 5.5. Next, Al₂O₃ NPs were added to the antibody solution and mixed under constant rotational stirring at room temperature for 30 min. The oxidation step results in the activation of the carbohydrate moieties present in the Gal-1 antibodies. The activated carboxyl group reacts with the amino group present on the silane modified alumina nanoparticles through covalent interaction, resulting in the formation of an amide bond. This allows the fragment crystallizable region (Fc) of the antibody to be bound to the nanoparticle surface while the fragment antigen binding region (Fab) is available during immunoassay. The Al₂O₃/Gal-1 nanoprobes were collected by centrifugation at 18,000 × g for 5 min and dispersed in milliprobe-DI water (conductivity and pH of the solution is 0.9 μS/cm and 5.5, respectively). Furthermore, we have also added the FTIR spectra in Fig. 2a for each step during nanoprobe synthesis. The absorption peak observed at 1080 cm⁻¹ can be assigned to the Si–O stretch after silane modification of the alumina nanoparticle surface while the broad peak observed at around 3500 cm⁻¹ can be assigned to the overlapping of primary amine and hydroxyl groups. The characteristic peak at 1625 cm⁻¹ and 1540 cm⁻¹ corresponds to the carbonyl stretch and the N–H stretch of the amide band, respectively, and confirms antibody conjugation to the surface modified alumina nanoparticles.

2.3. T24 cell lysate preparation

The human urinary bladder urothelial carcinoma T24 cell was obtained from the Bioresource collection and research center, Hsinchu, Taiwan and cultured at 37 °C in McCoy's5A medium [GIBCO (Life Technologies Corporation), Grand Island, N.Y., U.S.A.] supplemented with 10% fetal bovine serum. The T24 cell lysate was lysed and harvested using a mammalian protein extraction buffer (GE Healthcare) according to the manufacturer's suggestions. The protein concentration in the cell lysate was determined using the Bio-Rad DC protein assay kit. The original concentration of the T24 cell lysate was 0.25 mg/ml, which was collected with about 90% cell confluency. The immunosensor detection sensitivity was evaluated using six dilutions (0.25, 0.125, 0.0626, 0.03125, 0.01563 and 0.0078 mg/ml) of the original lysate in phosphate buffer saline (PBS) and in artificial urine. The artificial urine was synthesized according to a previously reported protocol (Brooks and Keevil, 1997) where 2.1 g of NaHCO₃, 10 g of CH₄N₂O, 5.2 g of NaCl, 3.2 g of Na₂SO₄, 1.3 g of NH₄Cl, 1 g of peptone (L37), 0.005 g of Yeast extract, 0.37 g of CaCl₂, 0.0012 g of FeSO₄, 0.49 g of MgSO₄, 0.95 g of KH₂PO₄ and 1.2 g of K₂PO₄ were mixed into a litre of DI water while the pH was adjusted to 7.2 using NaOH. Furthermore, the efficacy of immunosensor for actual urinary analysis has also been tested by comparing T24 spiked human urine samples

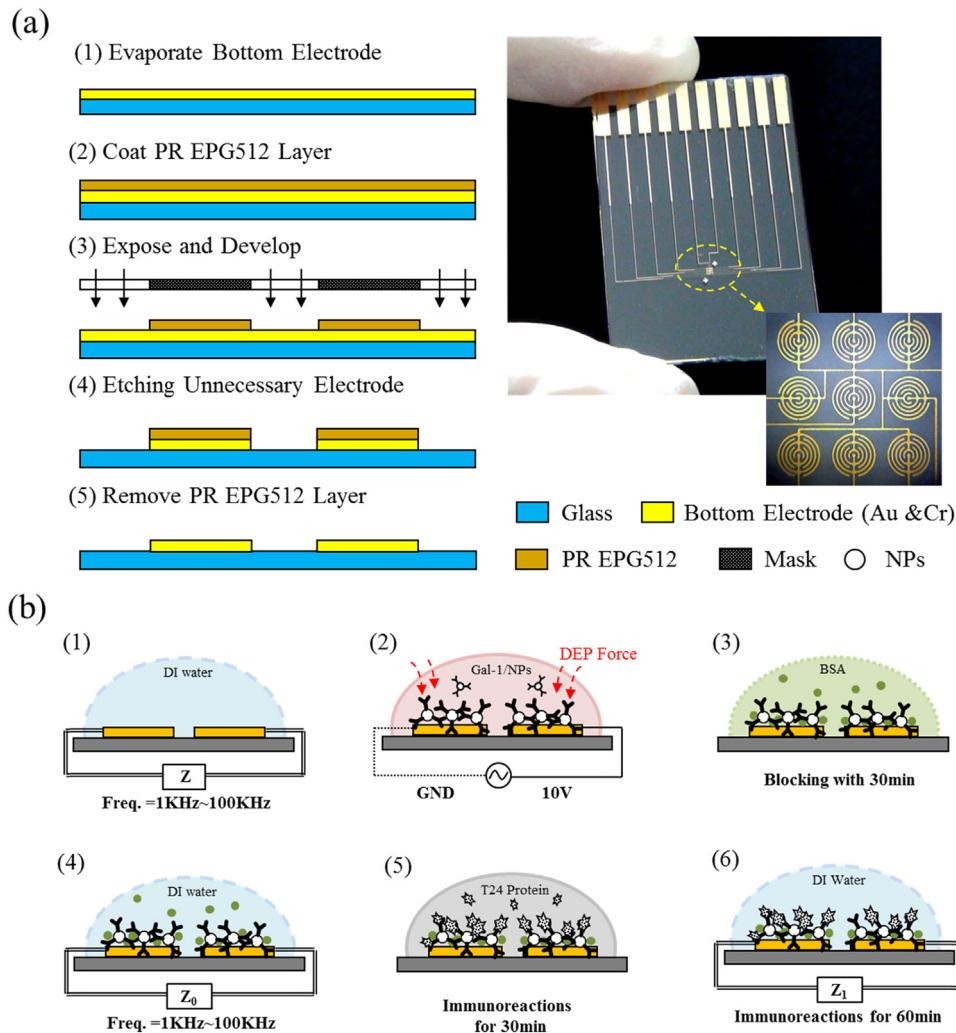


Fig. 1. (a) Schematic of the immunosensor fabrication process using standard photolithography. Also shown are an image of the finished immunosensor chip and an optical microscopy image of the 3×3 gold annular interdigitated microelectrode array. (b) Schematic of the different steps involved during operation of the immunosensor.

(0.03125 mg/ml) with unspiked samples while specificity can be determined by comparing the response observed for two different grade cancer cell lysates.

2.4. Immunosensor fabrication

A standard microfabrication process has been used for the fabrication of the immunosensor which has been schematically illustrated in Fig. 1a. First, a $40 \times 60 \text{ mm}^2$ microscope slide was ultrasonically cleaned using acetone and methanol solution for 5 min to remove any dust or organic pollutants. Next, 300 \AA of chromium (Cr) and 700 \AA of gold (Au) were evaporated sequentially onto the microscope slide using an electron beam physical vapor deposition (EBPVD) technique at a controlled temperature. A photoresist layer was then spin coated followed by masked exposure and a developing step to pattern the annular microelectrode array. The final steps involve wet etching of excess electrode and photoresist removal. The immunosensor consists of 9 interdigitated microelectrodes (3×3) with each electrode having a width and gap of $10 \mu\text{m}$ and a total sensing area of 0.64 mm^2 .

2.5. Operation mechanism

The immunosensor operation involves the trapping of the nanoparticles followed by antigen detection using electrochemical

impedance analysis and each step is schematically illustrated in greater detail in Fig. 1b. Impedance measurements were calibrated using an LCR meter (Wayne Kerr Electronics, WK 6420) with the data acquisition controlled by a computer-based LabVIEW program to scan the impedance spectrum in a frequency range of 1 kHz to 100 kHz. $100 \mu\text{l}$ of nanoprobe suspension is dropped onto the sensing area using a micropipette and an AC signal of $10 V_{pp}$ at 100 kHz is applied for 30 min using a function generator (AFG3022, Tektronix) to trap nanoparticles based on the p-DEP force. The immobilization of nanoparticles on the microelectrode surface after trapping can be observed in the optical microscopy images obtained using a CCD camera (XC10, Olympus) mounted on a biological microscope (BX51, Olympus) as shown in Fig. 2c. After the nanoparticles are trapped, we incubate with bovine serum albumin (BSA) solution for 30 min to effectively eliminate residual binding capacity and reduce non-specific interactions on the electrode surface and observe a higher signal to noise ratio due to the blocking step. BSA is selectively attached on the bare Au electrode surface via physical absorption and does not hinder the formation of an antigen-antibody complex during immunosensing. This is because the negatively charged BSA protein with an isoelectric point (pI) of 4.7 (Huang et al., 2015) in a solution of PBS (pH \sim 7.4) is electrostatically repelled by the negatively charged Gal-1 antibodies which have a pI of about 5.4 (Lutomski et al., 1996). In this way we can ensure that the impedance change after

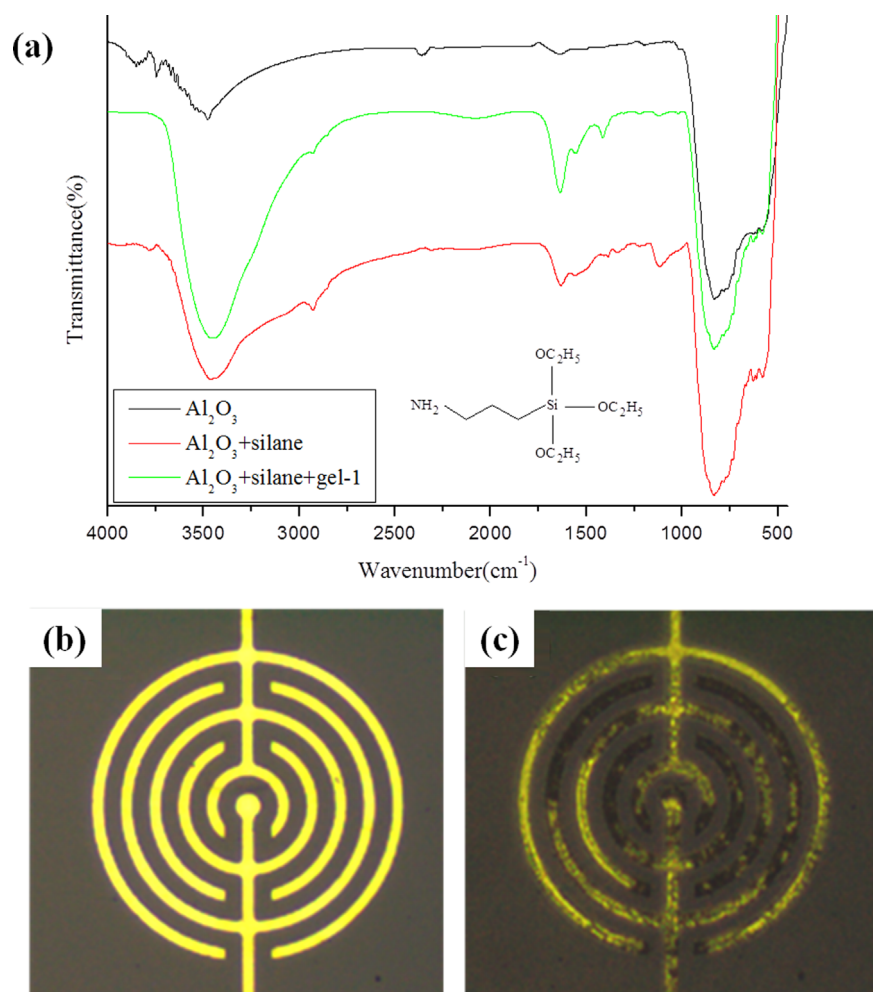


Fig. 2. (a) FTIR spectra for confirming the different steps utilized during nanoprobe synthesis. (b) OM image of bare microelectrode. (c) OM image of microelectrode after DEP trapping of nanoprobe.

immunosensing is because of the formation of antibody/antigen complex and not due to physical immobilization of proteins on the bare electrode surface. The blocking step is followed by washing with DI water and the baseline impedance before immunosensing is recorded (Z_0). Next, 100 μ l of spiked T24 cell lysate samples were dropped onto the sensing area and left for immunosensing for a further 30 min. This is followed by a washing step to remove any unbound proteins and the impedance after immunoassay is recorded (Z_1).

The impedance results for each step (bare electrode, after trapping and after immunosensing) were obtained in DI water. The impedance change (ΔZ) due to immunoreaction can be mathematically expressed as $Z_1 - Z_0$. 10 immunosensors have been used to test each concentration of cell lysate used. The error bars have been added and it can be seen that the results obtained are reproducible and reliable. We have tried to eliminate the differences in initial impedance observed at different electrodes which arises primarily due to their differing lengths by normalizing the impedance response during immunosensing (ΔZ) with the initial impedance observed after nanoprobe trapping and BSA blocking at that particular electrode (Z_0) and this is referred to as the normalized impedance variation ($\Delta Z/Z_0$). The normalized impedance variation has been calculated at an operating frequency of 10 kHz for which we observe the maximum stable response during immunosensing. While a larger response can be observed at lower frequencies (< 1 kHz), it shows lesser reproducibility and a lower signal to noise ratio as environmental conditions must be closely

monitored and controlled while performing immunosensing.

3. Results and discussion

3.1. Feasibility of immunosensor

To confirm the feasibility of the immunosensor, we did preliminary tests to detect Gal-1 in T24 cell lysate spiked PBS, a commonly used buffer solution whose ion concentration and osmolarity closely matches that of the human body, making it suitable for biological research. The impedance values obtained as a function of frequency for different steps during immunosensor operation have been plotted in Fig. 3a. The impedance increases by about 1.5 times at 10 kHz after nanoprobe trapping for 30 min using p-DEP. This is because the Al_2O_3 nanoparticles are dielectric and result in high baseline impedance, Z_0 . Next, a solution of spiked PBS (0.25 mg/ml) is incubated on the sensing area for 30 min and it was observed that the impedance increased a further 2 times after immunosensing. During immunoreaction, the Gal-1 proteins have a negative surface charge as the pH of PBS is 7.4 while the pI of Gal-1 is about 5.4. This would imply further accumulation of negative charges on the microelectrode surface after a stable antibody-antigen complex has formed. Consequently, the charge transfer resistance across the interdigitated microelectrodes through the solution increases, thus resulting in increased overall impedance. The ability to detect specific proteins

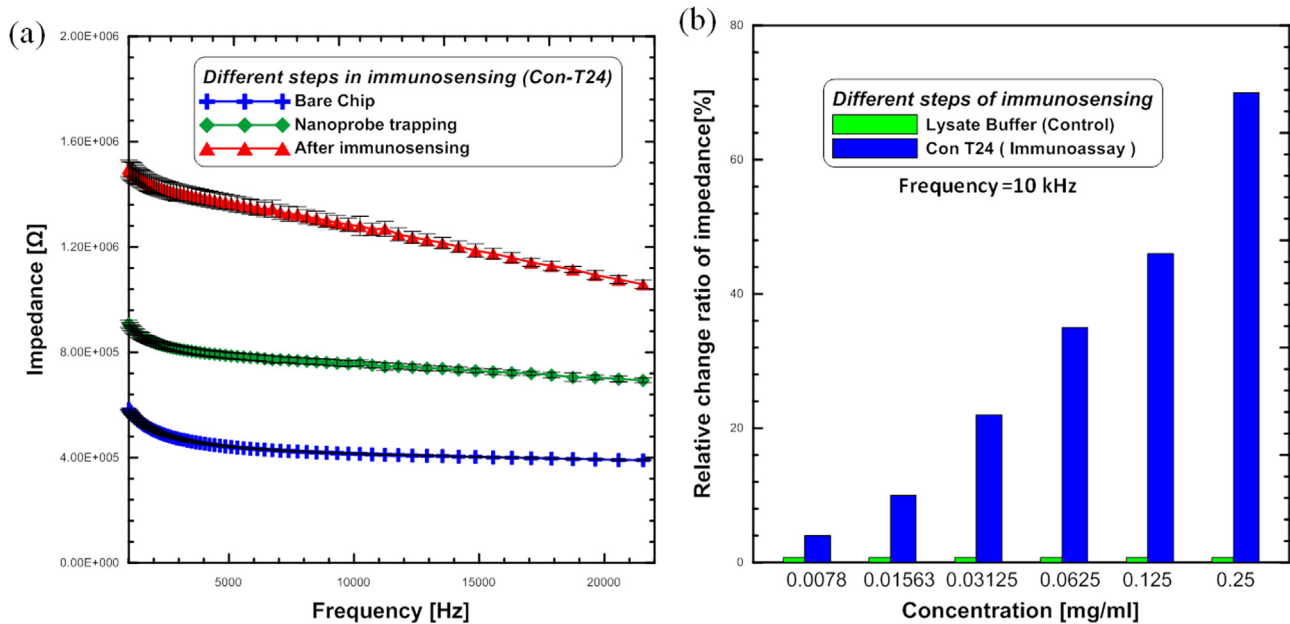


Fig. 3. (a) Impedance change as a function of frequency observed for different steps during immunoassay of T24 cell lysate in PBS (0.25 mg/ml). (b) The normalized impedance variation observed for different concentrations of T24 cell lysate show a linear dependence with a limit of detection of 0.0078 mg/ml. For the control samples, the impedance variation is almost negligible when no lysate is added to PBS.

like Gal-1 from a multitude of other proteins present in cell lysate highlights the selectivity of the immunosensor and is directly related to the nanoprobe immobilization efficiency. In other words, the concentration of trapped nanoprobe is enhanced by using p-DEP, resulting in amplified signals after immunosensing with cell lysate. It was also observed that the normalized impedance variations increase linearly as the concentration of cell lysate in PBS increases from 0.0078 to 0.25 mg/ml as shown in Fig. 3b. We have also tested the immunosensor with unspiked PBS which served as the control. It was observed that the normalized impedance variation for the lowest concentration of cell lysate used (0.0078 mg/ml) is about 4% which is more than 4 times higher than that observed for the control ($< 1\%$). The limit of detection (LOD) of the immunosensor is 0.0078 mg/ml or 7.8 $\mu\text{g/ml}$ of T24 cell lysate in PBS and urine samples. However T24 cell lysate is a complex fluid and contains a multitude of different proteins (calculated to be about $10^4/\text{cell}$) (Ron, 2013) including Gal-1. Thus the actual limit of detection of the immunosensor for Gal-1 could be estimated to be in the pg/ml range. However, to ensure that the immunosensor is specific for Gal-1 among the many proteins present in T24 cell lysate, we have compared the immunosensor response for the same concentration (0.0325 mg/ml) of two different grades of bladder cancer cell lysates (see Supplementary information). The normalized impedance variation after immunosensing with T24 (Grade III) cell lysate is 17.1% which is significantly higher than the 1.3% observed for the RT4 (Grade I) cell lysate. To further confirm our results, we have used western blot to first isolate the Gal-1 protein based on its molecular weight using gel electrophoresis followed by immunoreaction with Gal-1 antibody. We observe a dark band at 14 kDa (molecular weight of Gal-1) when T24 cell lysate is used while no response is observed for RT4 cell lysate and our results are in agreement with those obtained in literature (Lutomski et al., 1996; Ron, 2013; Liao et al., 2011). This shows that Gal-1 protein present in T24 cell lysate specifically takes part in immunosensing to form a stable complex with the Gal-1 antibody. The sensitivity of immunosensor, defined as the normalized impedance variation dependence on concentration of T24 cell lysate present (slope of the calibration curve), is about 6.44 times/mg $^{-1}$ ml $^{-1}$. Thus, the immunosensor

chip shows feasibility for sensitive, specific and quantitative detection of Gal-1.

3.2. Detection of Gal-1 in spiked artificial and human urine

Since detection of bladder cancer is performed using urinary analysis, we have tested the efficacy of the immunosensor for detection of Gal-1 in T24 lysate spiked artificial and human urine samples as shown in Fig. 4 while unspiked samples are used as control. The normalized impedance variations increase linearly as the concentration of lysate in artificial urine increases from 0.0078 to 0.25 mg/ml. The highest observed variation is about 56% for the spiked sample (0.25 mg/ml) while that for the control at the same concentration is only 0.69%. It was also observed that the ratio of impedance variations for test and control sites is highest at 76 times (0.25 mg/ml) and lowest at 15 times (0.0078 mg/ml), thus demonstrating a linear behavior. The immunosensor also showed significant increase in normalized impedance variations for human urine samples that have been spiked with 0.03125 mg/ml T24 cell lysate with highest and lowest variations of about 54% and 23%, respectively, while the highest variation in control samples is only about 1%. It is interesting to note that the impedance increases ($Z_1 > Z_0$) after immunosensing with spiked PBS while it decreases ($Z_0 > Z_1$) for spiked artificial and human urine samples. We propose that this might be related to the significantly higher ionic strength of urine samples as compared to PBS. Since all the impedance measurements are made in DI water without the presence of a redox probe, the capacitive effects (modelled as the series combination of the surface modification capacitance and the double layer capacitance) dominate as charge transfer resistance approaches infinity. This explains why the impedance increases after trapping of dielectric alumina nanoprobe as this results in an increase in the surface modification capacitance. During immunoreaction, the Gal-1 antigen-antibody complex is negatively charged in spiked PBS (pH=7.2) and urine samples (pH=6.8–7.2) as explained in the previous section. The accumulation of negative charges on the electrode surface (increase in capacitance) combined with the low ionic strength of PBS (0.01 M) hinders electron transfer across the interdigitated electrodes, resulting in an

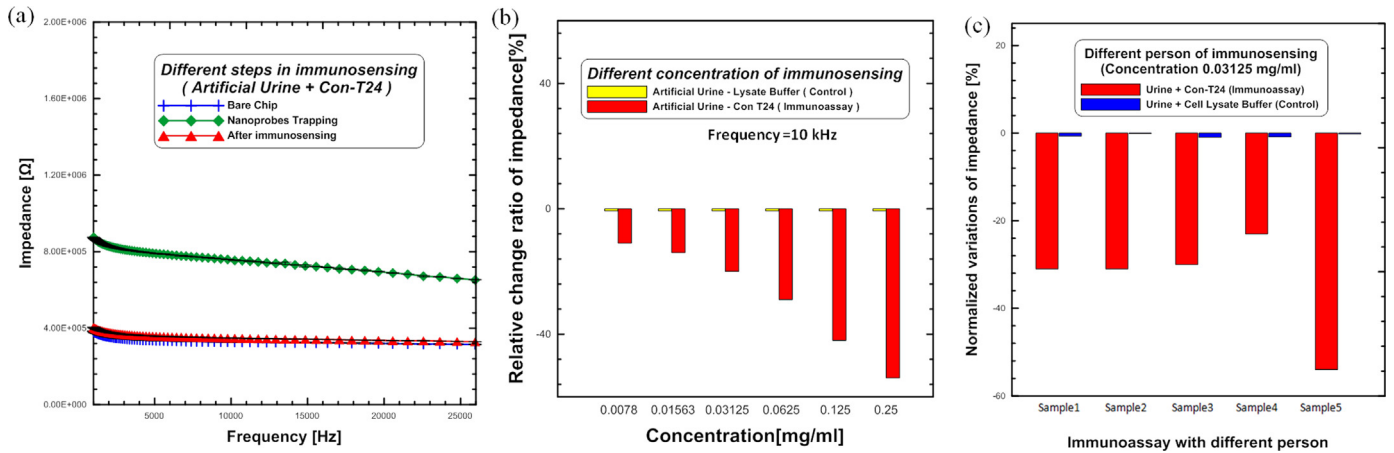


Fig. 4. (a) Impedance change as a function of frequency observed for different steps during immunoassay of T24 cell lysate in artificial urine (0.25 mg/ml). (b) Normalized impedance variations for artificial urine spiked with different concentrations of T24 cell lysate (test) and unspiked (control). (c) Normalized impedance variations for human urine spiked with 0.03125 mg/ml of T24 cell lysate (test) and unspiked (control).

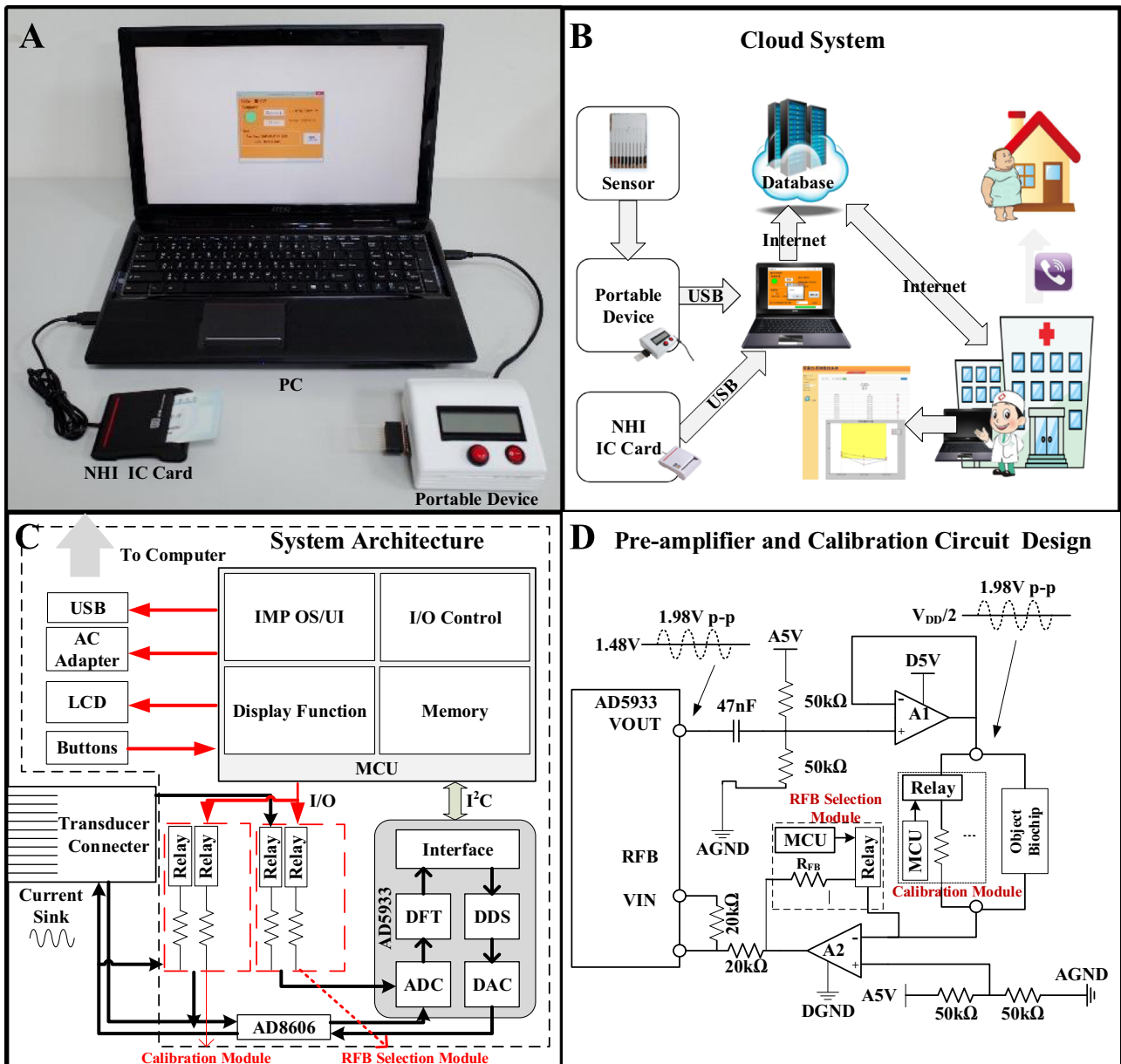


Fig. 5. (a) An image of the point of care system which includes the immunosensor chip attached to the portable device for impedance measurement, a National Health Insurance (NHI) IC Card reader and personal computer. (b) A schematic of data collection and transmission to cloud data base. (c) Block diagram of portable impedance measuring device. (d) Design of pre-amplifier and calibration circuit to improve accuracy and stability by increased signal-noise ratio (SNR) during impedance analysis.

increase in impedance after immunosensing. On the other hand, the notably higher ionic strength (0.8–1 M) of urine enables positive ions to be electrostatically attracted to the negative charges on the electrode surface, thus reducing the overall surface capacitance. Furthermore, these residual positive ions are difficult to wash away and act as holes that facilitate charge transfer leakage across the interdigitated microelectrodes, resulting in reduction in overall impedance after immunosensing. The proposed immunosensor shows high sensitivity and specificity for Gal-1 detection in artificial and human urine samples. The next step will involve clinical testing of urinary samples of patients suffering from bladder cancer and this research is in progress and results will be published in the near future.

3.3. Use in point of care testing

In order for the immunosensor to be applicable for quantitative point of care testing, certain prerequisites have to be satisfied. These include a chip centered device for immunoassay of complex fluids and a miniaturized self-containing readout device. The major challenges in achieving this goal is creating an easy to operate chip, which does not require complicated fluid circuits and micro fabricated valves and pumps, and the lack of versatile portable detection systems. In order for the immunosensor to meet the requirements of point of care, the impedance analysis must be performed using a portable impedance analyzing device rather than the LCR meter which is often used in laboratory settings. Therefore, we have designed a prototype of a portable impedance device that can operate in a frequency range of 1 kHz to 100 kHz as shown in Fig. 5. It is based on an AD5933 integrated circuit (IC) where the response signal from the impedance is sampled by the on-board ADC and a discrete Fourier transform (DFT) and communicated to a digital microcontroller through an I²C interface. Self-calibration functions were implemented by four sets of switching relays and precision resistors. The device can calculate optimal gain values before measurement to avoid errors due to environmental factors such as humidity or temperature. A smart gain function allows the device to automatically switch gain resistors to find the best fit for the immunosensor chip. In this way, we could achieve a wide range of impedance measurements without manual control. We have compared impedance measurements of the portable impedance device with an LCR meter at an operating frequency of 10 kHz and have obtained results with a maximum deviation of 3.47% (see Supplementary information). The results obtained using the portable device can be read on the liquid crystal display (LCD) with two buttons to interface with the user. All the data including the date, patient's information and measured results from portable analyzer can be uploaded to the patients file on the internet using a National Health Insurance (NHI) IC Card, USB connection and a personal computer. The doctor can then view the uploaded results and can directly contact the patient if further examination is required.

4. Conclusions

In summary, we have developed an immunosensor chip for the rapid, sensitive and quantitative detection of Gal-1 protein in T24 cell lysate spiked samples. The chip utilizes a photolithographically patterned highly stable gold microelectrode array which allows for

ultrasensitive detection while only using 100 μ l of sample volume. We have used p-DEP manipulations to improve nanoprobe immobilization on the microelectrode surface and have also designed a miniaturized impedance analyzer. While the immunosensor chip attached to this portable read out device can be used in the field, at home or even in resource limited settings, the ability to transfer the data for cloud computing should allow for improved monitoring of public health and clinical analysis.

Acknowledgments

The authors would like to thank the National Science Council of the Republic of China, Taiwan, for financially supporting this research under Contract no. MOST 103-2218-E-218-001. The Nanotechnology Research Center and Roll-to-Roll Imprinting Technology Alliance for Flexible Optoelectronics of Southern Taiwan University of Science and Technology is commended for providing the MEMS facilities.

Appendix A. Supplementary material

Supplementary data associated with this article can be found in the online version at <http://dx.doi.org/10.1016/j.bios.2015.12.103>.

References

- Brooks, T., Keevil, C.W., 1997. *Lett. Appl. Microbiol.* 24, 203–206.
- Chikkaveeraiiah, B.V., Bhirde, A.A., Morgan, N.Y., Eden, H.S., Chen, X., 2012. *ACS Nano* 6, 6546–6561.
- Chuang, C.H., Wu, T.F., Chen, C.H., Chang, K.C., Ju, J.W., Huang, Y.W., Nhan, V.V., 2015. *Lab. Chip* 15, 3056–3064.
- Daniels, J.S., Pourmand, N., 2007. *Electroanalysis* 19, 1239–1257.
- Drummond, T.G., Hill, M.G., Barton, J.K., 2003. *Nat. Biotechnol.* 21, 1192.
- Elshafey, R., Tavares, A.C., Sij, M., Zourob, M., 2013. *Biosens. Bioelectron.* 50, 143–149.
- Hirsh, S.L., Bilek, M.M.M., Nosworthy, N.J., Kondyurin, A., Dos Remedios, C.G., McKenzie, D.R., 2010. *Langmuir* 26, 14380–14388.
- Harrington, M.S., Anderson, L.B., 1990. *Anal. Chem.* 62, 546–550.
- Huang, J., Lin, L., Sun, D., Chen, H., Yang, D., Li, Q., 2015. *Chem. Soc. Rev.* 44, 6330–6374.
- Lisdat, F., Schafer, D., 2008. *Anal. Bioanal. Chem.* 391, 1555–1567.
- Li, Y., Afrasiabi, R., Fathi, F., Wang, N., Xiang, C., Love, R., et al., 2014. *Biosens. Bioelectron.* 58, 193–199.
- Luo, X., Davis, J.J., 2013. *Chem. Soc. Rev.* 42, 5944–5962.
- Lutomski, D., Caron, M., Cornillot, J.D., Bourin, P., Dupuy, C., Pontet, M., Bladier, D., Joubert-Caron, R., 1996. *Electrophoresis* 17, 600–606.
- Liao, L.C., Li, C.F., Shen, K.H., Chien, L.H., Huang, H.Y., Wu, T.F., 2011. *Pathology* 43 (7), 707–712.
- Ma, H., Wallbank, R.W.R., Chaji, R., Li, J., Suzuki, Y., Jiggins, C., 2013. *Sci. Rep.* 3, Ploeg, M., Aben, K.K.H., Kiemeny, L.A., 2009. *World J. Urol.* 27, 289–293.
- Park, S.J., Taton, T.A., Mirkin, C.A., 2002. *Science* 295, 1503–1506.
- Rodriguez, M.C., Kawde, A.N., Wang, J., 2005. *Chem. Commun.*, 4267–4269.
- Radke, S.M., Alcolija, E.C., 2005. *Biosens. Bioelectron.*, 1662–1667.
- Ron, Milo, 2013. *Bioessays*. 35 (12), 1050–1055.
- Singh, R., Suni, I.L., 2010. *J. Electrochem. Soc.* 157, J334–J337.
- Shi, W.T., Ma, Z.F., 2011. *Biosens. Bioelectron.* 26, 3068–3071.
- Thévenot, D.R., Toth, K., Durst, R.A., Wilson, G.S., 2001. *Biosens. Bioelectron.* 16, 121–131.
- Wlodkowic, D., Cooper, J.M., 2010. *Anal. Bioanal. Chem.*, 193–209.
- Wu, T.F., Li, C.F., Chien, L.H., Shen, K.H., Huang, H.Y., Su, C.C., Liao, A.C., 2015. *J. Urol.* 193 (3), 909–915.
- Yutkin, V., Nisman, B., Pode, D., 2010. *Expert Rev. Anticancer Ther.* 10, 787–790.
- Zheng, G., Patolsky, F., Cui, Y., Wang, W.U., Lieber, C.M., 2005. *Nat. Biotechnol.* 23, 1294–1301.
- Zhang, C., Khoshmanesh, K., Mitchell, A., Kalantar-Zadeh, K., 2010. *Anal. Bioanal. Chem.* 396 (1), 401–420.